Search for excited quarks with the ATLAS experiment at the CERN LHC: W/Z+jet channel

O. Çakır
Ankara University, Faculty of Sciences, Department of Physics, 06100, Tandogan, Ankara, Turkey

C. Leroy and R. Mehdiyev*
Université de Montréal, Département de Physique, Montréal (Québec), Canada H3C 3J7

(Received 12 December 2000; published 4 April 2001)

Resonant production of excited quarks at the CERN LHC by the quark gluon fusion process and their subsequent decay to ordinary quarks and weak gauge bosons W and Z is investigated. Event selection cuts are applied to separate the signal from background. At an integrated luminosity of $3\times10^5\ \mathrm{pb}^{-1}$, the mass reaches of 7 TeV for qW, and 4.5 TeV for qZ channel are achieved.

DOI: 10.1103/PhysRevD.63.094014 PACS number(s): 13.85.Rm, 13.87.Ce, 14.80.−j

I. INTRODUCTION

A consequence of a possible substructure of quarks is the existence of excited quarks $q^\star$ with masses of the order of the compositeness scale Λ. Excited quarks have been discussed in Refs. [1,2], and several types of experimental limits on masses and couplings have been obtained [3–5]. The Collider Defector at Fermilab (CDF) [4] and D0 [5] Collaborations have excluded the mass region below 540 GeV for both photon+jet (γj) and W+jet (Wj) decay channels and excluded the mass region $80<m^\star<570$ GeV using the dijet (jj) channel. More recently, mass ranges $200<m^\star<520$ GeV and $580<m^\star<760$ GeV for excited quarks in the double jets channel have been excluded by CDF [6]. The D0 Collaboration has excluded the mass region $200<m^\star<720$ GeV for all channels [5].

Excited quarks can be produced in pp collisions at the CERN Large Hadron Collider (LHC) via quark-gluon fusion. They decay to a quark by emitting any gauge boson (g, γ, W, or Z). The masses of the excited quarks are assumed to be at least of the order of the compositeness scale Λ. An effective Lagrangian of the magnetic moment type, describing transition between an excited quark of mass $m^\star$ and the common quarks q is constrained by gauge invariance to be [2]

$$L=\frac{1}{2\Lambda}\overline{q}^\star_R\sigma^{\mu\nu}\left(g_s f_s\frac{\lambda_a}{2}G^a_{\mu\nu}+gf\frac{\tau}{2}W_{\mu\nu}+g'f'\frac{Y}{2}B_{\mu\nu}\right)q_L+\mathrm{H.c.},\quad(1)$$

where G^a, W, and B are the field-strength tensors for the SU(3), SU(2), and U(1) gauge fields, respectively; λ_a, τ, and Y are the corresponding gauge structure constants; g_s, g, and g' are the corresponding gauge coupling constants. Finally, f_s, f, and f' are the couplings determined by the compositeness dynamics.

Excited quarks can be searched for in the invariant mass spectrum of the decay products, if the lowest excited states of the spectrum are kinematically reachable. The signals for singly produced excited quarks are the large transverse momentum jj, γj, Wj, or Zj pairs with an invariant mass peaking at $m^\star$.

This work is a continuation of previous works devoted to the study of the excited quark production with subsequent decay to a quark and photon [7] and to a quark and gluon [8]. In the present paper, the quark+W/Z decay mode is investigated. If the excited quarks are sufficiently heavy, $m^\star>m_{W,Z}$, they can decay into a quark q and an intermediate weak vector boson W or Z with the following decay widths ($V=W,Z$):

$$\Gamma(q^\star\to qV)=\frac{1}{8}\frac{g_V^2}{4\pi}f_V^2\frac{m^{\star3}}{\Lambda^2}\left(1-\frac{m_V^2}{m^{\star2}}\right)^2\left(2+\frac{m_V^2}{m^{\star2}}\right),\quad(2)$$

where $f_Z=fT_3\cos^2\theta_W-f'(Y/2)\sin^2\theta_W$ and $f_W=f/\sqrt{2}$ with T_3 and Y being the third component of the weak isospin and the weak hypercharge of the excited quark $q^\star$, respectively. $g_W=g_e/\sin\theta_W$ ($g_e=\sqrt{4\pi\alpha}$) and $g_Z=g_W/\cos\theta_W$ are the standard model W and Z coupling constants, respectively. m_V is the mass of the weak gauge boson W or Z. The Feynman diagrams for the processes $ug\to u^\star\to dW\to df\bar{f}'$ or $dg\to d^\star\to uW\to uf\bar{f}'$ and $ug\to u^\star\to uZ\to uf\bar{f}$ or $dg\to d^\star\to dZ\to df\bar{f}$ are considered and shown in Figs. 1(a) and 1(b).

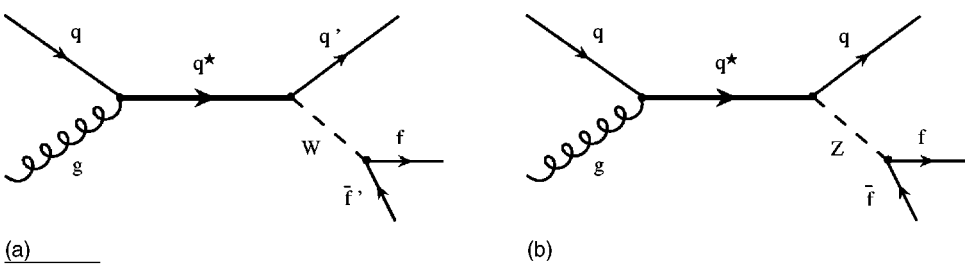

FIG. 1. Feynman graphs for the excited quark production via the $qg\to q^\star\to q'W\to q'f\bar{f}'$ (a) and $qg\to q^\star\to qZ\to qf\bar{f}$ (b) processes.

*On leave of absence from Institute of Physics, Azerbaijan Academy of Sciences, 370143, Baku, Azerbaijan.

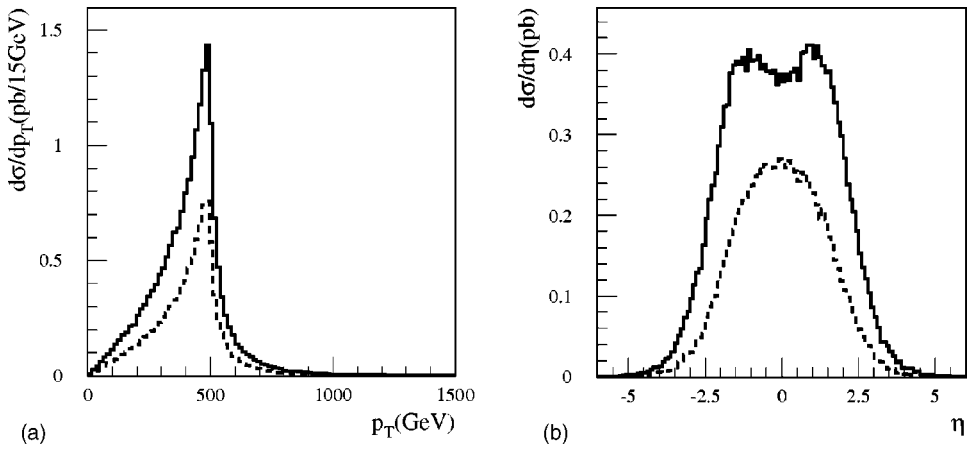

FIG. 2. The transverse momentum (a) and pseudorapidity (b) distributions for the excited quark signal (qW channel) with the scale $\Lambda = m^\star = 1$ TeV and couplings $f = f_s = 1$. Solid and dashed lines represent the d-quark and u-quark distributions, respectively.

II. SIMULATION

In this work, only the first generation of excited quarks $u^\star$ and $d^\star$ was simulated for the excited quark signal. For a comparison with the other decay channels, the decay widths Γ of the excited quarks into ordinary quarks plus gauge bosons g, W, Z, γ and the relative branching ratios BR, obtained from PYTHIA [9], are given in Table I for the excited quark masses $m^\star = 1,3,5$ TeV and for the couplings $f = f' = f_s = 1$, taking $\Lambda = m^\star$. The decay widths of excited quarks to weak gauge bosons plus ordinary quarks represent ~15% of the total decay width.

The simulation of the excited quark signal (quark and W or Z) and relevant backgrounds was performed with ATLFAST [10] to take into account the experimental conditions prevailing at LHC for the ATLAS detector [11]. The hadronic calorimeters were used to reconstruct the energy of jets in cells of dimensions $\Delta\eta \times \Delta\phi = 0.1 \times 0.1$ within the pseudorapidity range $-2.5 < \eta < 2.5$, where ϕ is the azimuthal angle. The hadronic energy resolution is given by $0.5/\sqrt{E(\mathrm{GeV})} \oplus 0.03$ over this η region. Hadronic showers are regarded as jets when they lie within a cone of radius $\Delta R = 0.7$ and possess a transverse energy $E_T > 15$ GeV.

The electromagnetic calorimeters were used to reconstruct the energy of leptons in cells of dimensions $\Delta\eta \times \Delta\phi = 0.025 \times 0.025$ within the same pseudorapidity range $-2.5 < \eta < 2.5$. The electromagnetic energy resolution is given by $0.1/\sqrt{E(\mathrm{GeV})} \oplus 0.0005$ over this η region. Electromagnetic showers are identified as leptons when they lie within a cone of radius $\Delta R = 0.1$ and possess a transverse energy $E_T > 5$ GeV. Lepton isolation criteria were applied. They require a distance $\Delta R > 0.4$ from other clusters and a maximum transverse energy $E_T < 10$ GeV deposition in cells in a cone of radius $\Delta R = 0.2$ around the electron emission direction. This study is restricted to the calometric facilities to investigate both jet and lepton mode of W/Z decays.

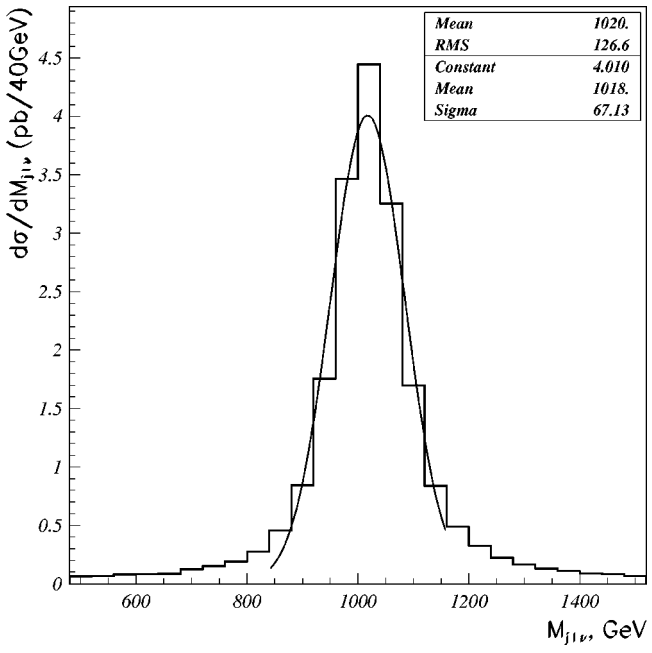

FIG. 3. The distribution of the reconstructed mass of jet+lepton+neutrino system $m(jl\nu)$, for the excited quark mass $\Lambda = m^\star = 1$ TeV and couplings $f = f_s = 1$.

A. $q'W$ channel

Partonic level information from PYTHIA for the decay products of the excited quarks is shown in Fig. 2 (qW channel). As can be seen from Fig. 2, the jets in the signal events have high transverse momenta (~415 GeV) in the midrapidity region. The signal for $u^\star$ production is roughly twice as large as for $d^\star$ due to the parton distributions in the proton. In this case, the events including d quark accompanied with W^+ boson is dominating over uW^- final state at the partonic level. The transverse momentum distributions have a maximum at half the mass the of excited quarks. Therefore, p_T and η cuts could help to eliminate the corresponding backgrounds.

Signal and backgrounds lead to 3-jet events or 1-jet+1 lepton +1 neutrino events. The main background for these signal processes comes from single production of W/Z particles which produces a large number of jets originating from processes such as $W/Z \rightarrow 2$ jets. Processes which involve the production of W and Z bosons (with their subsequent decay

TABLE I. The total decay width Γ of the excited quarks into ordinary quarks and gauge bosons $V=g,W,Z,\gamma$, and relative branching ratios $\mathrm{BR}=\Gamma(q^\star\to qV)/\Sigma_V\Gamma(q^\star\to qV)$ for $\Lambda=m^\star$ and $f=f'=f_s=1$.

	$m^\star=1$ TeV		$m^\star=3$ TeV		$m^\star=5$ TeV	
Decay mode	Γ (GeV)	BR	Γ (GeV)	BR	Γ (GeV)	BR
$d^\star\to$all	37.31	1.0	102.1	1.0	163.8	1.0
$d^\star\to dg$	30.86	0.8271	82.35	0.806	130.6	0.797
$d^\star\to uW^-$	4.257	0.1141	13.05	0.128	21.89	0.134
$d^\star\to dZ^0$	1.975	0.0529	6.07	0.059	10.18	0.062
$d^\star\to d\gamma$	0.222	0.0059	0.67	0.007	1.129	0.007
$u^\star\to$all	37.32	1.0	102.1	1.0	163.8	1.0
$u^\star\to ug$	30.86	0.8269	82.35	0.806	130.6	0.797
$u^\star\to dW^+$	4.257	0.1141	13.05	0.128	21.89	0.134
$u^\star\to uZ^0$	1.318	0.03532	4.05	0.040	6.796	0.042
$u^\star\to u\gamma$	0.8864	0.02375	2.69	0.026	4.515	0.028

TABLE II. The cross section×branching ratio (in pb) for the signal $q'W$ at partonic level for excited quark masses 1000–7000 GeV. The values are given for the scale $\Lambda=m^\star$ and for various couplings $f=f_s$.

$f\backslash m^\star$ (GeV)	1000	2000	3000	5000	7000
1.0	29.92	1.10	9.87×10^{-2}	1.66×10^{-3}	3.11×10^{-5}
0.5	7.55	2.80×10^{-1}	2.52×10^{-2}	4.16×10^{-4}	7.12×10^{-6}
0.1	3.03×10^{-1}	1.12×10^{-2}	1.01×10^{-3}	1.67×10^{-5}	2.83×10^{-7}

TABLE III. The cross section×branching ratio (in pb) for the backgrounds to the $q'W$ process at partonic level for various $\hat{p}_T$ ranges and the average transverse momentum values $\langle\hat{p}_T\rangle$.

$\hat{p}_T$ (GeV)	$\langle\hat{p}_T\rangle$ (GeV)	$W+$jet backg.	$W+W$ backg.	$W+Z$ backg.
$100<\hat{p}_T<300$	194	91.30	6.31×10^{-1}	1.23×10^{-1}
$300<\hat{p}_T<600$	377	6.94	9.13×10^{-2}	1.14×10^{-2}
$600<\hat{p}_T<1000$	713	0.30	2.11×10^{-2}	5.99×10^{-4}
$1000<\hat{p}_T<1600$	1135	1.88×10^{-2}	8.81×10^{-3}	4.25×10^{-5}
$\hat{p}_T>1600$	1370	7.60×10^{-4}	2.28×10^{-3}	1.80×10^{-6}

TABLE IV. The cross section×branching ratios (in pb) for the signal $q^\star\to qZ$ at partonic level for excited quarks masses 1000–7000 GeV. The values are given for the scale $\Lambda=m^\star$ and various couplings $f=f'=f_s$.

$f\backslash m^\star$ (GeV)	1000	2000	3000	5000	7000
1.0	3.39	1.22×10^{-1}	1.08×10^{-2}	1.78×10^{-4}	3.27×10^{-6}
0.5	8.54×10^{-1}	3.10×10^{-2}	2.75×10^{-3}	4.44×10^{-5}	7.49×10^{-7}
0.1	3.409×10^{-2}	1.250×10^{-3}	1.106×10^{-4}	1.781×10^{-6}	2.962×10^{-8}

TABLE V. The cross section×branching ratios (in pb) from PYTHIA for the backgrounds to the $q^\star\to qZ$ process and the average transverse momentum values $\langle\hat{p}_T\rangle$.

$\hat{p}_T$ (GeV)	$\langle p_T\rangle$ (GeV)	$Z+$jet backg.	$Z+W$ backg.	$Z+\gamma$ backg.
$150<\hat{p}_T<300$	195	12.5	3.680×10^{-2}	2.739×10^{-2}
$300<\hat{p}_T<600$	376	9.872×10^{-1}	3.442×10^{-3}	2.709×10^{-3}
$600<\hat{p}_T<1000$	713	4.314×10^{-2}	1.798×10^{-4}	1.560×10^{-4}
$1000<\hat{p}_T<1600$	1135	2.672×10^{-3}	1.273×10^{-5}	1.156×10^{-5}
$\hat{p}_T>1600$	1371	1.065×10^{-4}	5.393×10^{-7}	5.154×10^{-7}

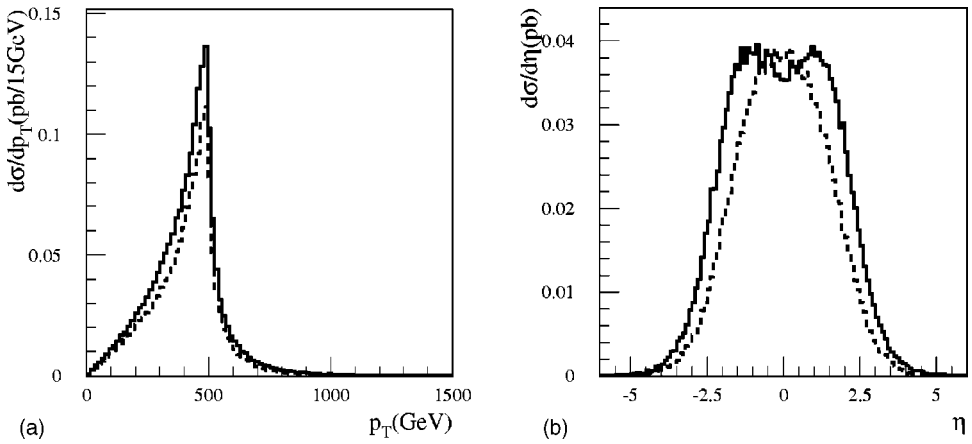

FIG. 4. The transverse momentum (a) and pseudorapidity (b) distributions for the excited quark signal (qZ channel) with the scale $\Lambda = m^\star = 1$ TeV and couplings $f = f' = f_s = 1$. Solid and dashed lines represent the u- and d-quark distributions, respectively.

to leptons) were analyzed. Since the background dominates over the $q^\star$ signal in the 3-jet channel, we have selected only W bosons which decay leptonically into electrons or muons with high transverse momentum $p_T > 30$ GeV and event missing transverse energy $E_T > 50$ GeV. The lepton was required to have $|\eta| < 2.5$ and to be separated from any nearby jets by $\Delta R > 0.4$ in $\eta - \phi$ space. The longitudinal neutrino momentum p_z, in the decay of a W, has been constrained to give an $l\nu$ invariant mass equal to the W boson mass of 80 GeV (W mass constraint).

The effective mass distributions of the $jl\nu$ system obtained from ATLFAST for $m^\star = 1000$ GeV are shown in Fig. 3. One can note that the width of the mass distribution for this channel is smaller than the double jets channel from the previous study [8].

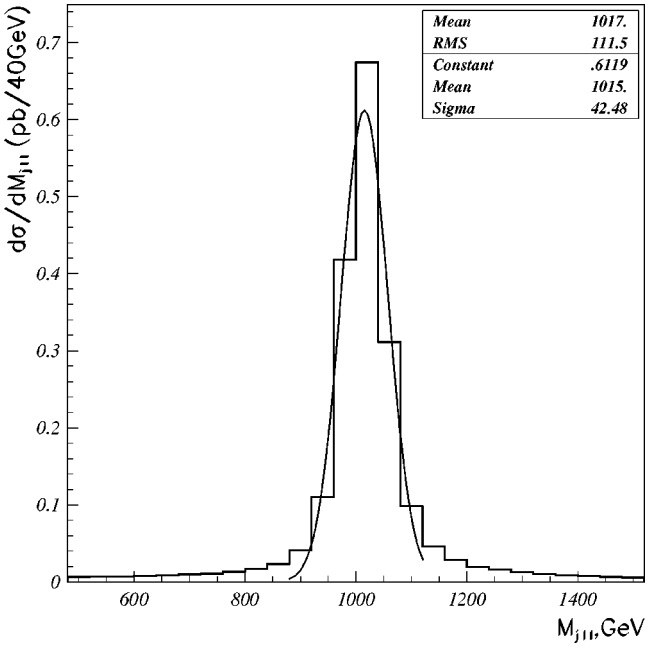

FIG. 5. The distribution of the reconstructed mass of jet+2 leptons system $m(jl^+l^-)$, for the excited quark mass $\Lambda = m^\star = 1$ TeV and coupling $f = f' = 1$.

The relevant signal and background cross-sections are presented in Tables II and III, respectively. Here the background contributions from the lowest order W+jet production and WW and WZ processes (the second W or Z is assumed to decay to jets, and one of the jets is missed out of acceptance).

B. $q^\star \to qZ$ channel

Partonic level information from PYTHIA for the decay products of the excited quarks is shown in Fig. 4 (qZ channel). As can be seen from Fig. 4, the jets in the signal events have high transverse momenta ($\sim$415 GeV) in the midrapidity region. The signal for $u^\star$ production is roughly twice as large as for $d^\star$ due to the parton distributions in the proton. However, the square of the couplings of Z boson to d-type quarks is stronger than to u-type quarks by a factor of 1.5 [see Eq. (2), and also Table I]. Therefore, the contributions from the u and d quark final state to the p_T and η distribution are approximately the same for this channel. The transverse momentum distributions have a maximum at half the mass of the excited quarks. These could be helpful to eliminate the corresponding backgrounds.

The signal and backgrounds lead to 3-jet events or 2-lepton+1 jet events. Since the background dominates over the $q^\star$ signal in the 3-jet channel, we have selected only Z bosons which decay leptonically into two leptons with high transverse momentum $p_T > 30$ GeV. The lepton was required to have $|\eta| < 2.5$ and to be separated from any nearby jets by $\Delta R > 0.4$ in $\eta - \phi$ space. The reconstructed jll invariant mass distribution obtained from ATLFAST for $m^\star = 1$ TeV is shown in Fig. 5. The width of the jll mass distribution is smaller than for $jl\nu$ events as one expects from Eq. (2). The relevant signal and background cross sections are presented in Tables IV and V, respectively. The CTEQ [12] parton distribution functions for the signal and background calculations have been used. Here the contributions to the background come from lowest order Z+jet production, Z+photon (if γ is energetic and misidentified from jet), and ZW (if W decays to jets and one of the jets is missed out of acceptance).

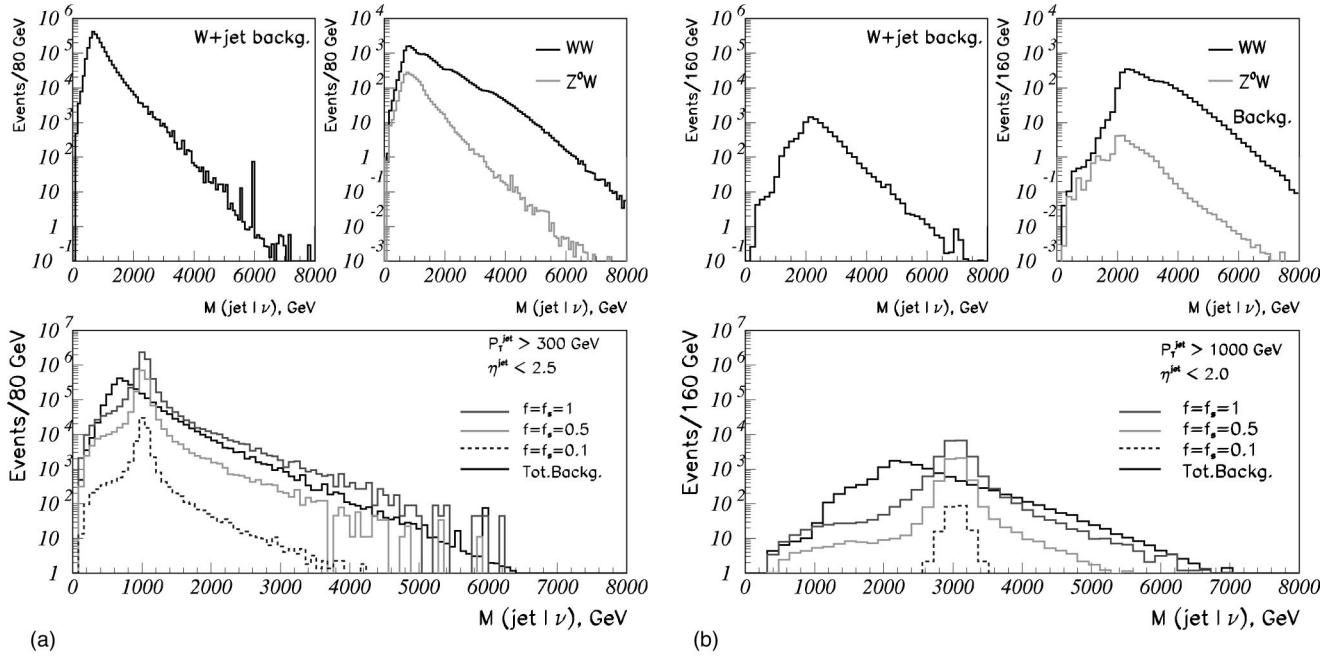

FIG. 6. Distributions of the reconstructed mass of jet+lepton+neutrino system for the backgrounds and for the excited quark mass of 1 TeV (a) and 3 TeV (b) (qW decay), with cuts and couplings indicated. The distributions are normalized to an intergral luminosity $L=3\times10^5\ \mathrm{pb}^{-1}$.

III. RESULTS

The production cross sections for the excited quarks are given in Tables II and IV. The following cuts were used to separate the signal from the background.

The transverse momentum of jet was required to be at least $p_T>300\,\mathrm{GeV}$ (for $m^\star=1000\,\mathrm{GeV}$) and increased for higher $m^\star$. Minimum transverse momentum cuts were chosen to be around $m^\star/2-\delta p_T$, where δp_T was optimized for each $m^\star$.

The pseudorapidity interval $|\eta|<2.5$ is chosen ($|\eta|<2.0$ for $m^\star>3000\,\mathrm{GeV}$ and beyond).

The resulting differential cross sections $d\sigma/dm_{jlv}$ for the

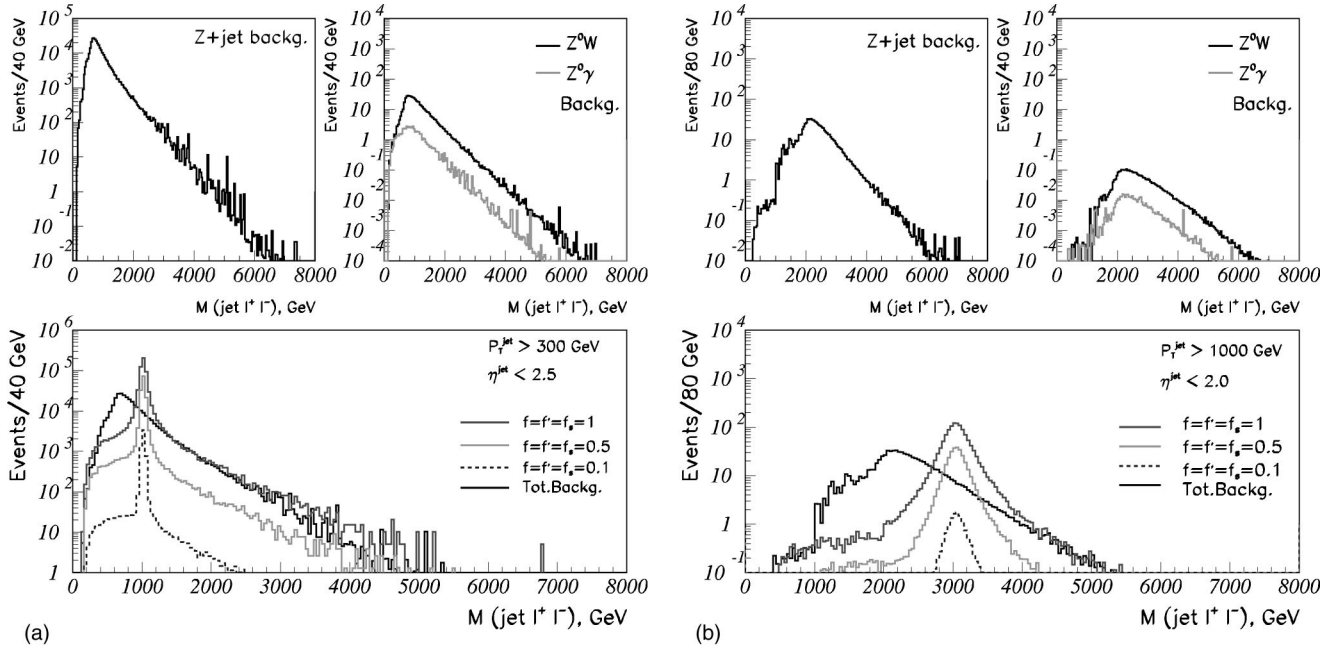

FIG. 7. Distributions of the reconstructed mass of jet+2 leptons system for the backgrounds and the excited quark mass of 1 TeV (a) and 3 TeV (b) (qZ decay), with cuts and couplings indicated. The distributions are normalized to an integated luminosity $L=3\times10^5\ \mathrm{pb}^{-1}$.

TABLE VI. Number of events for both signal (S) and background (B), and signal significance $S/\sqrt{B}$ are calculated for the windows $\Delta m_{jl\nu}$ around the excited quark mass peak for $\Lambda = m^\star$ and various couplings $f = f_s$ at an integrated luminosity $L = 3 \times 10^5\ \mathrm{pb}^{-1}$.

$m^\star$ (GeV)	$f(f_s)$	$\Delta m_{jl\nu}$ (GeV)	S	B	$S/\sqrt{B}$
	1.0	269	4833000	425250	7411.30
1000	0.5	228	1261200	356250	2113.03
	0.1	213	51003	322500	89.81
	1.0	452	206350	14760	1698.48
2000	0.5	362	54408	11940	497.92
	0.1	338	2250	10560	21.89
	1.0	588	17626	1125	525.50
3000	0.5	493	4837	954	156.60
	0.1	461	197	870	6.68
	1.0	921	329	13	90.97
5000	0.5	786	86	11	25.93
	0.1	733	4	10	1.26
7000	1.0	1324	5	1	5.00
	0.5	1036	1.5	0.4	2.37

excited quark mass $m^\star = 1000$ and 3000 GeV with the corresponding backgrounds are given in Fig. 6 (qW decay). The distributions were normalized to an integrated luminosity of $3 \times 10^5\ \mathrm{pb}^{-1}$.

The resulting differential cross section $d\sigma/dm_{jll}$ distributions for the excited quark mass $m^\star = 1000$ and 3000 GeV with the corresponding backgrounds are given in Fig. 7 (qZ decay). The same normalization as for Fig. 6 was applied.

The mass bin width selection for all mass distributions is made for the signal and the backgrounds according to the width of the corresponding mass distribution at each mass value. The jlv and jll invariant mass distributions are integrated around the excited quark masses for different mass bin window Δm to obtain the signal and background number of events.

TABLE VII. Number of events for both signal (S) and background (B), and signal significance $S/\sqrt{B}$ are calculated for the windows Δm_{jll} around the excited quark mass peak for $\Lambda = m^\star$ and various couplings $f = f' = f_s$ at an integrated luminosity $L = 3 \times 10^5\ \mathrm{pb}^{-1}$.

$m^\star$ (GeV)	$f(f')$	Δm_{jll} (GeV)	S	B	$S/\sqrt{B}$
	1.0	170	465990	417000	721.62
1000	0.5	122	126410	313500	225.77
	0.1	106	5209	261750	10.18
	1.0	350	15694	1185	463.75
2000	0.5	249	4112	885	138.22
	0.1	229	168	735	6.19
	1.0	654	1079	116	100.18
3000	0.5	518	281	93	29.14
	0.1	486	11	85	0.30
5000	1.0	1400	13	25	2.60
	0.5	1159	5	19	1.15

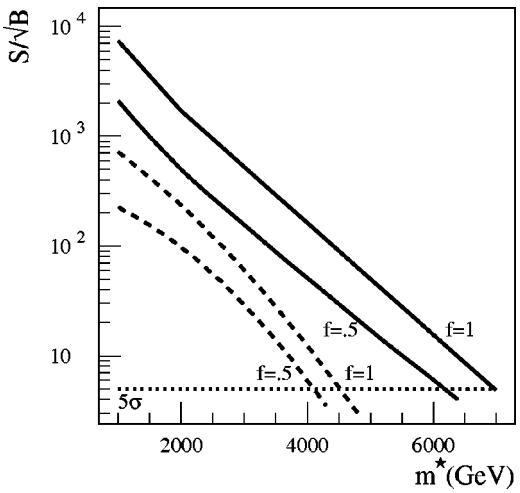

FIG. 8. Excited quark signal significance for $q^\star \to qW$ channel (solid lines) and $q^\star \to qZ$ channel (dashed lines) at the integrated luminosity of $3 \times 10^5\ \mathrm{pb}^{-1}$ at LHC.

The number of events for both signal (S) and background (B), and the signal significance ($S/\sqrt{B}$) are presented in Tables VI and VII for qW and qZ excited quark decay channels (and various couplings), respectively.

The signal significance is defined at each mass point as $S/\sqrt{B}$ where S and B are the number of accepted signal and background events in the selected mass bin, respectively. Achievable mass limits for the relevant channels of the excited quark decay are established by requiring the criteria $S/\sqrt{B} > 5$ and at least 10 signal events within the cuts per year, which corresponds to a 99% confidence level (C.L.).

The signal significance at each mass point for the channels qW and qZ are shown in Fig. 8. As can be seen from this plot the masses achieved for excited quarks in the qW mode are 7 TeV for the coupling $f = f_s = 1$ and 6.2 TeV for $f = f_s = 0.5$ for an integrated luminosity of $3 \times 10^5\ \mathrm{pb}^{-1}$ at CERN LHC. The corresponding masses for qZ channel are 4.5 and 4.1 TeV for the couplings $f = f' = f_s = 1$ and $f = f' = f_s = 0.5$, respectively.

IV. CONCLUSION

Excited quarks can be produced with large cross section in the resonance channel at LHC. The production of excited quarks was evaluated in the framework of a composite model and their subsequent decay of the excited quarks to qW or qZ final state were examined. The mass reach achievable at LHC is 7 TeV for qW channel, and 4.5 TeV for qZ channel at the integrated luminosity of $3 \times 10^5\ \mathrm{pb}^{-1}$, for the couplings $f = f' = f_s = 1$.

ACKNOWLEDGMENTS

We would like to thank G. Azuelos, D. Froidevaux, I. Hinchliffe, and L. Poggioli for their comments about the subject. C.L. and R.M. thank NSERC/Canada for their support.

[1] H. Terazawa *et al.*, Phys. Lett. **112B**, 387 (1982); F. M. Renard, Nuovo Cimento A **77**, 1 (1983); A. De Rujula, L. Maiani, and R. Petronzio, Phys. Lett. **140B**, 253 (1984).
[2] U. Baur, I. Hinchliffe, and D. Zeppenfeld, Int. J. Mod. Phys. A **2**, 1285 (1987); U. Baur, M. Spira, and P. M. Zerwas, Phys. Rev. D **42**, 815 (1990).
[3] UA2 Collaboration, J. Alitti *et al.*, Nucl. Phys. **B400**, 3 (1993).
[4] CDF Collaboration, F. Abe *et al.*, Phys. Rev. Lett. **72**, 3004 (1994); **74**, 3538 (1995).
[5] D0 Collaboration, I. Bertram, Report No. Fermilab-Conf-96/389-E, 1996.
[6] CDF Collaboration, F. Abe *et al.*, Phys. Rev. D **55**, R5263 (1997).
[7] O. Çakır and R. Mehdiyev, Phys. Rev. D **60**, 034004 (1999).
[8] O. Çakır, C. Leroy, and R. Mehdiyev, Phys. Rev. D **62**, 114018 (2000).
[9] T. Sjostrand, Comput. Phys. Commun. **82**, 74 (1994).
[10] E. Richter-Was, D. Froidevaux, and L. Poggioli, ATLAS Internal Note No. ATLAS-PHYS-98-131, 1998.
[11] ATLAS Collaboration, Technical Proposal, Report No. CERN/LHCC/94-43.
[12] CTEQ Collaboration, J. Botts *et al.*, Phys. Lett. B **304**, 159 (1993).